

MARSHALL ISLANDS FILE TRACKING DOCUMENT

Record Number: 319

File Name (TITLE): Further Radiation Studies  
of the High Energy Fission Products

Document Number (ID): UCRL-5087

DATE: 1/1958

Previous Location (FROM): LLNL

AUTHOR: Stevenson, et al

Additional Information: \_\_\_\_\_  
\_\_\_\_\_  
\_\_\_\_\_

OrMIbox: 18

CyMIbox: 11

UNIVERSITY OF CALIFORNIA  
Radiation Laboratory, Livermore Site  
Livermore, California

Contract No. W-7405-eng-48

FURTHER RADIOCHEMICAL STUDIES OF THE  
HIGH-ENERGY FISSION PRODUCTS

P. C. Stevenson, H. G. Hicks, W. E. Nervik, and D. R. Nethaway  
January 13, 1958

FURTHER RADIOCHEMICAL STUDIES OF THE HIGH-ENERGY  
FISSION PRODUCTS\*

P. C. Stevenson, H. G. Hicks, W. E. Nervik, and D. R. Nethaway

University of California Radiation Laboratory  
Livermore Site

January 13, 1958

ABSTRACT

Formation cross sections of various  $U^{238}$  fission products have been measured as a function of bombarding-particle energy, using protons (10-340 Mev) and deuterons (20-190 Mev). The reactions  $Al^{27}(p, 3pn)Na^{24}$  and  $Al^{27}(d, ap)Na^{24}$  were used as monitoring reactions to measure effective cyclotron beam intensity. Fission-product distribution curves and total fission cross sections have been measured. Above 50-Mev bombarding energy, the fission-product distribution is not symmetrical about a given mass number at a given bombardment energy.

---

\* This work was performed under the auspices of the U. S. Atomic Energy Commission.

## FURTHER RADIOCHEMICAL STUDIES OF THE HIGH-ENERGY FISSION PRODUCTS

P. C. Stevenson, H. G. Hicks, W. E. Nervik, and D. R. Nethaway

University of California Radiation Laboratory  
Livermore Site

January 13, 1958

### I. INTRODUCTION

Previous studies<sup>1,2</sup> of the high-energy charged-particle fission of  $U^{238}$  did not include examination of the yields of masses greater than 140. Formation cross sections of several rare-earth nuclides ( $A = 140$  to 157),  $Y^{90}$ ,  $Y^{91}$ ,  $Y^{93}$ ,  $Mo^{99}$ , and  $Ba^{140}$  have been measured in the present work. Proton energies range from 10 to 340 Mev; deuteron energies, from 20 to 190 Mev.

### II. EXPERIMENTAL TECHNIQUES

Preparation of targets<sup>3</sup> and bombardment techniques<sup>1</sup> have been described previously by some of the authors. The cyclotron beam intensity was monitored using the reactions  $Al^{27}(p, 3pn)Na^{24}$  (70 to 340 Mev) or  $Al^{27}(d, ap)Na^{24}$  (28 to 190 Mev) in aluminum foils surrounding the targets, as described previously;<sup>1,2,3</sup> the published cross sections of Hicks, Stevenson, and Nervik<sup>3</sup> and of Batzel, Crane, and O'Kelly,<sup>4</sup> were used. Beam intensities were measured by means of a Faraday cup when bombardments were made using 10- and 32-Mev protons and 20-Mev deuterons.

Radiochemical determination of  $Mo^{99}$  was performed in the manner described by Gunn et al.,<sup>5</sup> and the method of isolation and separation of

---

<sup>1</sup> H. G. Hicks, P. C. Stevenson, R. S. Gilbert, and W. H. Hutchin, Phys. Rev. 100, 1284 (1955).

<sup>2</sup> H. G. Hicks and R. S. Gilbert, Phys. Rev. 100, 1286 (1955).

<sup>3</sup> Hicks, Stevenson, and Nervik, Phys. Rev. 102, 1390 (1956).

<sup>4</sup> Batzel, Crane and O'Kelly, Phys. Rev. 91, 939 (1953).

<sup>5</sup> Gunn, Hicks, Stevenson, Levy, Phys. Rev. 107, 1642 (1957).

rare earths and yttrium was performed in the manner described by Nervik.<sup>6</sup> The Ba<sup>140</sup> was purified by repeated precipitation of the chloride from diethyl ether-hydrochloric acid mixtures and by scavenging with ferric and lanthanum hydroxides.

Gamma and bremsstrahlung radiations from all nuclides measured, except Mo<sup>99</sup>, were counted by means of a NaI(Tl) scintillation crystal, with the lower discriminator set at 20 kev and the upper discriminator set at 3 Mev. Sufficient beryllium (2g/cm<sup>2</sup>) to stop all beta particles was interposed between the counting sample and crystal. The counting of the gamma and bremsstrahlung radiations by-passed the problem of beta scattering, for experiments have shown that under these conditions there is no significant variation of observed specific activity with mass thickness of sample. The counting efficiency of each nuclide was determined by relating the observed counting rate of a carrier-free sample in the scintillation crystal counters to that in a 4π-geometry beta counter. Several determinations were made for each species and the agreement between duplicate determinations was excellent.

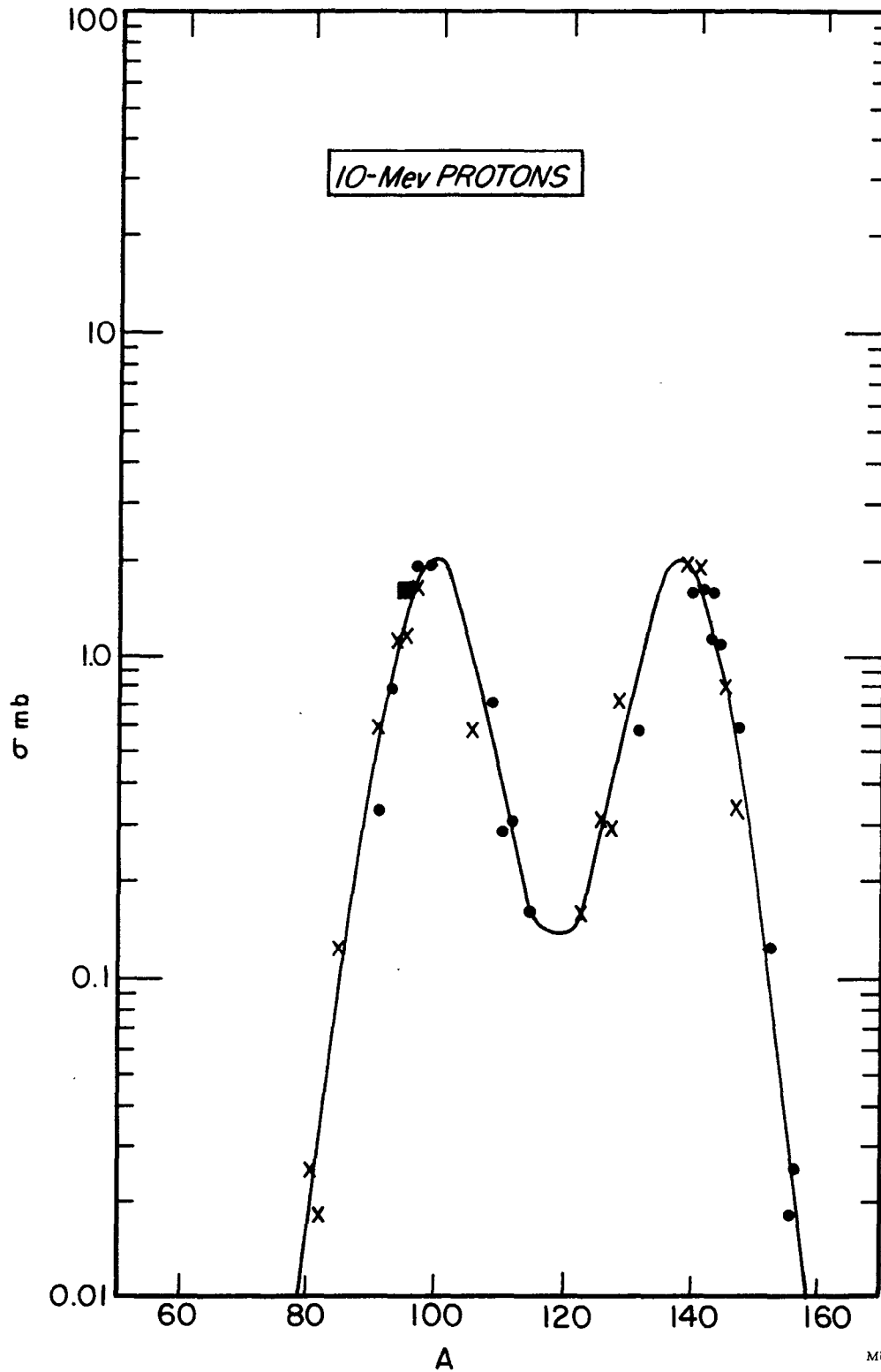
The nuclide Mo<sup>99</sup> was counted with an end-window, continuous-flow methane proportional counter. The counting efficiency was determined indirectly by means of fission counting (described in reference 5) and the accepted thermal-neutron fission yield of Mo<sup>99</sup>, 6.14%.<sup>7</sup> The formation cross sections are summarized in Figs. 1 and 2 and Tables I and II. The agreement with previous data<sup>1, 2, 8</sup> is good.

---

<sup>6</sup>W. E. Nervik, J. Phys. Chem. 59, 690 (1955).

<sup>7</sup>J. O. Blomeke, Oak Ridge Natl. Lab. Report No. ORNL-1783, Nov. 2, 1955.

<sup>8</sup>M. Lindner and R. N. Osborne, Phys. Rev. 94, 1323 (1954).



MUL-4263

Fig. 1 A. 10-Mev Protons

Fig. 1. Fission-product distributions of  $U^{238}$  bombarded with protons of various energies. The symbol ● denotes present work; ■ denotes previous work by Hicks, Stevenson, Gilbert and Hutchin;<sup>1,2</sup> ▲ denotes work by Lindner and Osborne;<sup>8</sup> and x denotes reflection points.

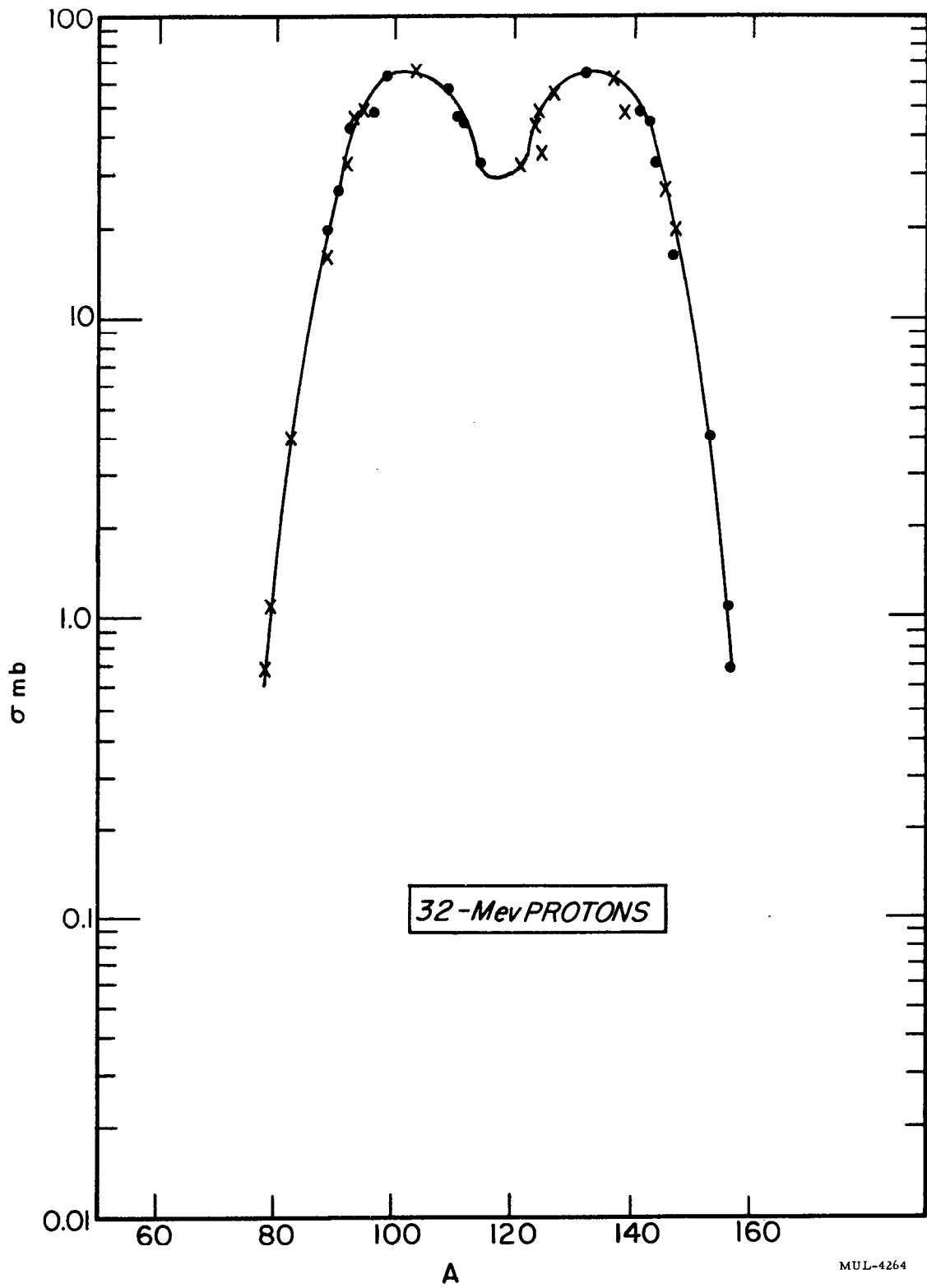


Fig. 1 B. 32-Mev Protons

MUL-4264

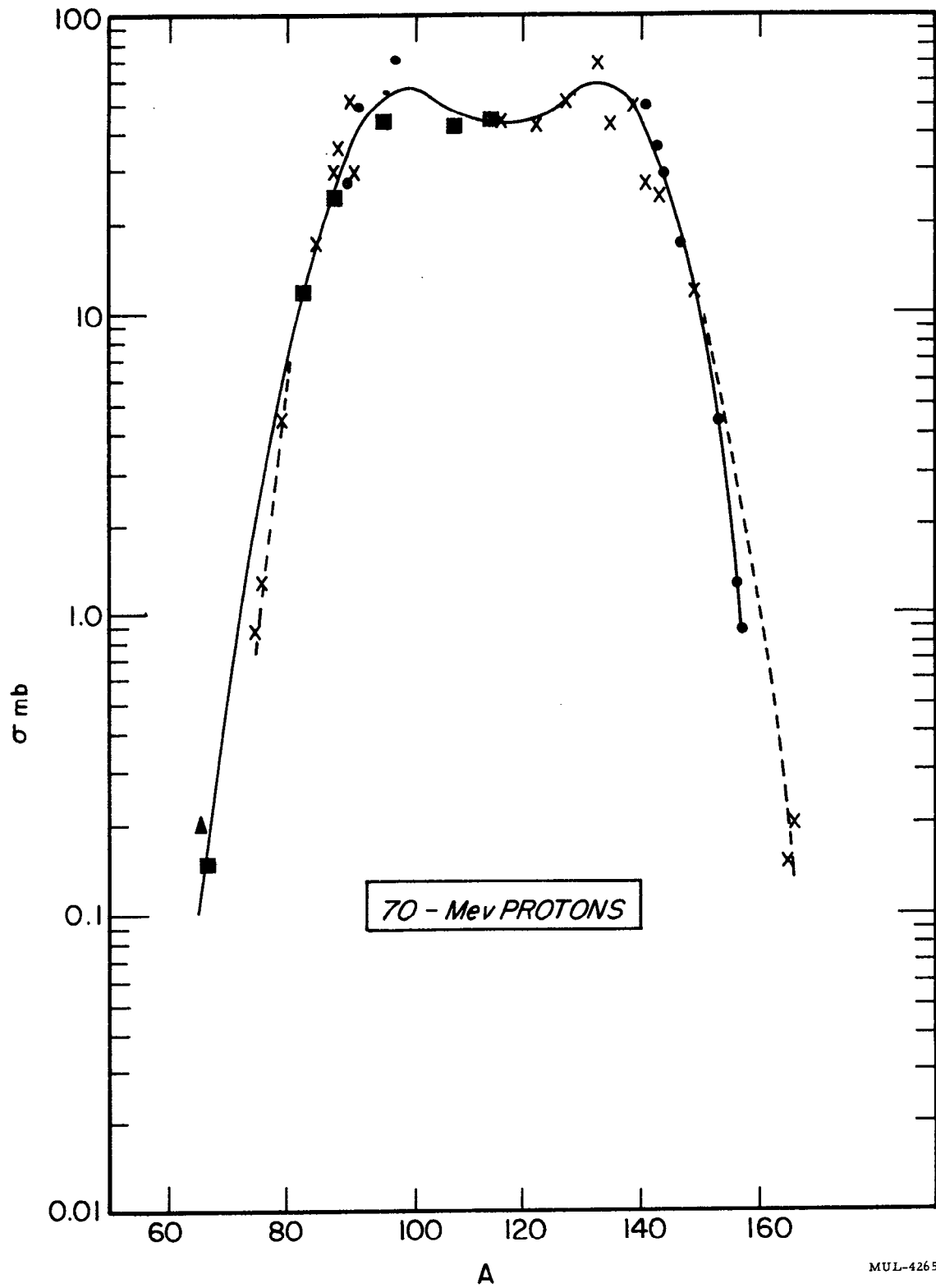


Fig. 1 C. 70-Mev Protons

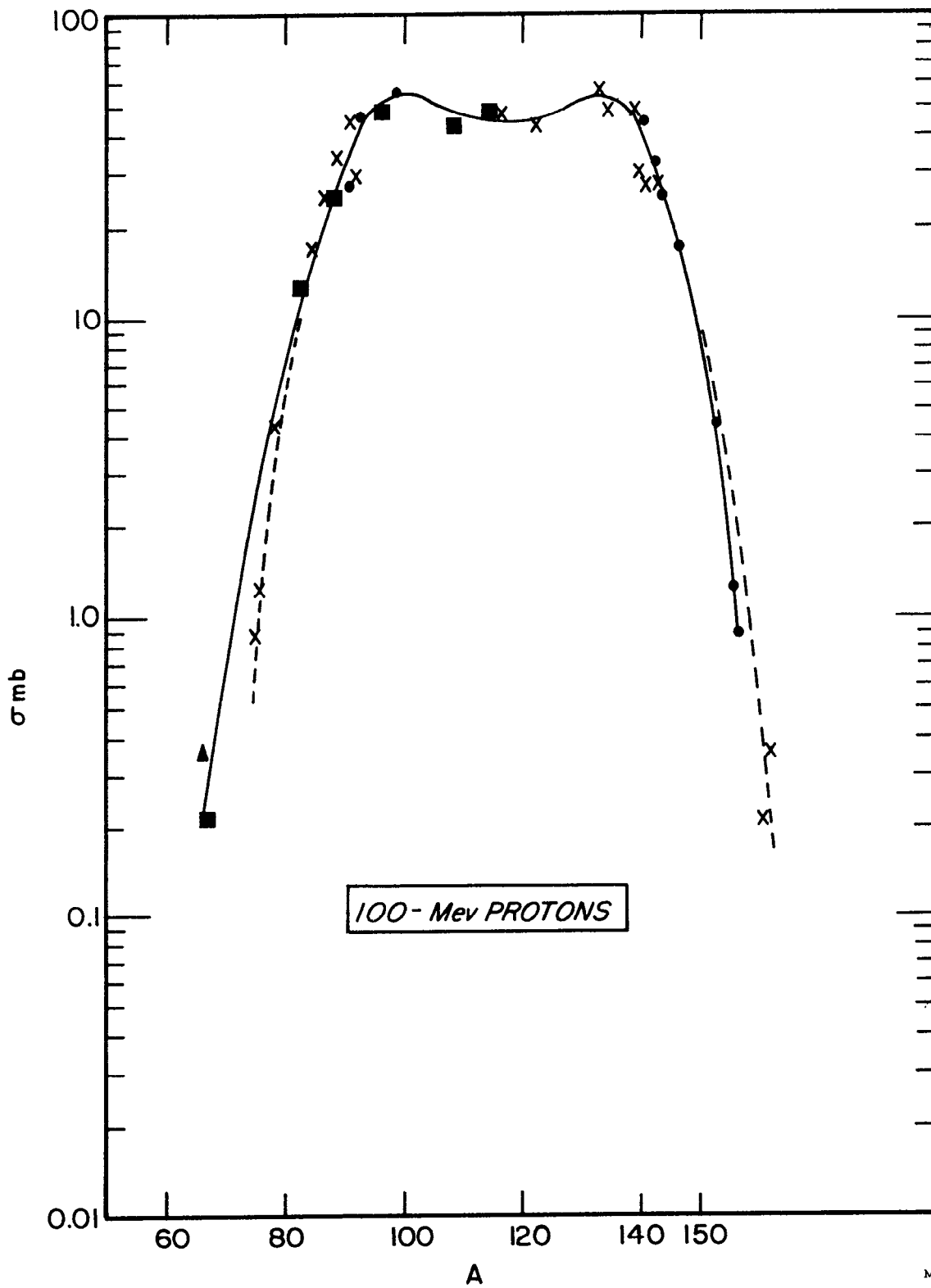


Fig. 1 D. 100-Mev Protons

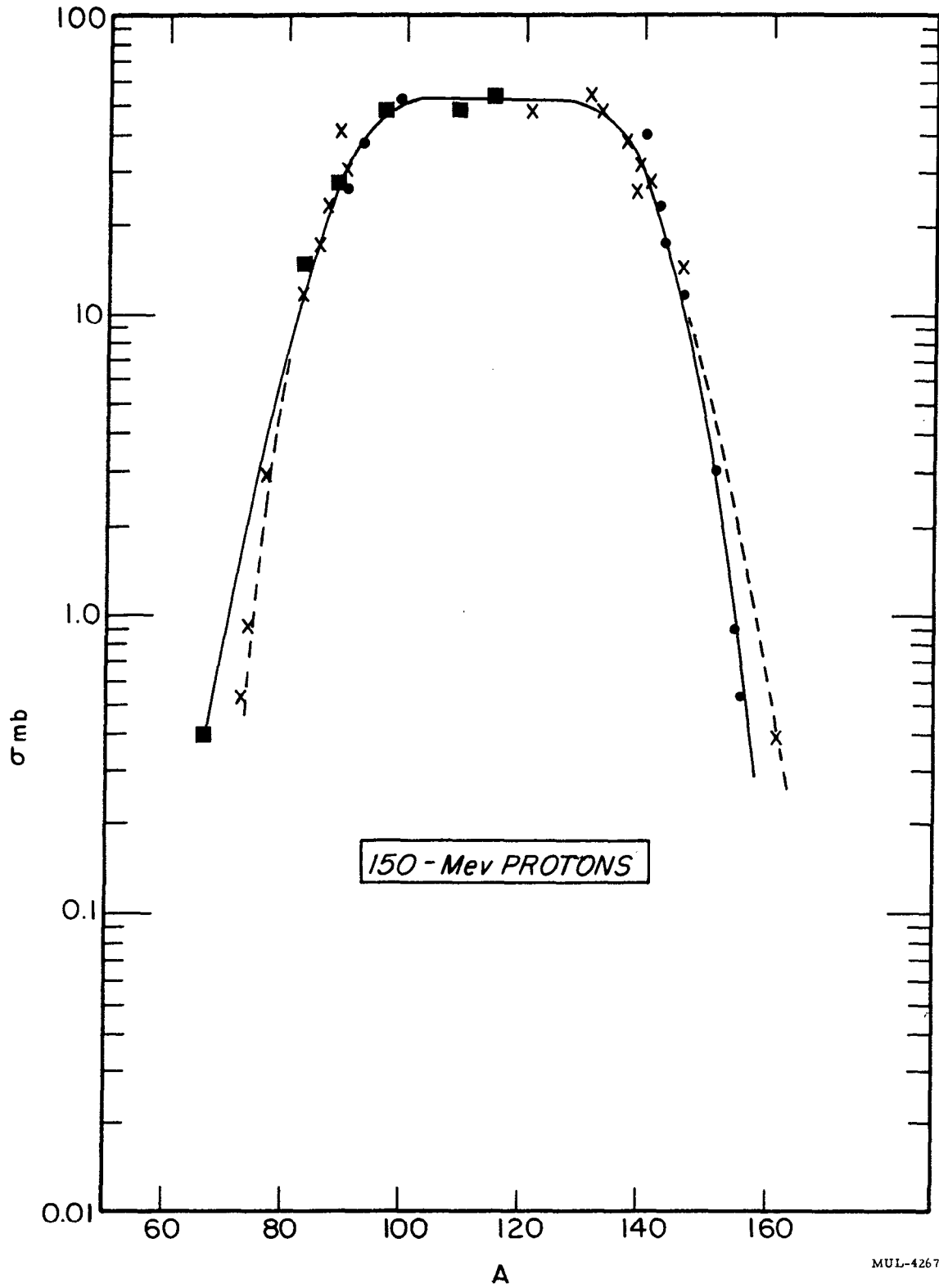


Fig. 1 E. 150-Mev Protons

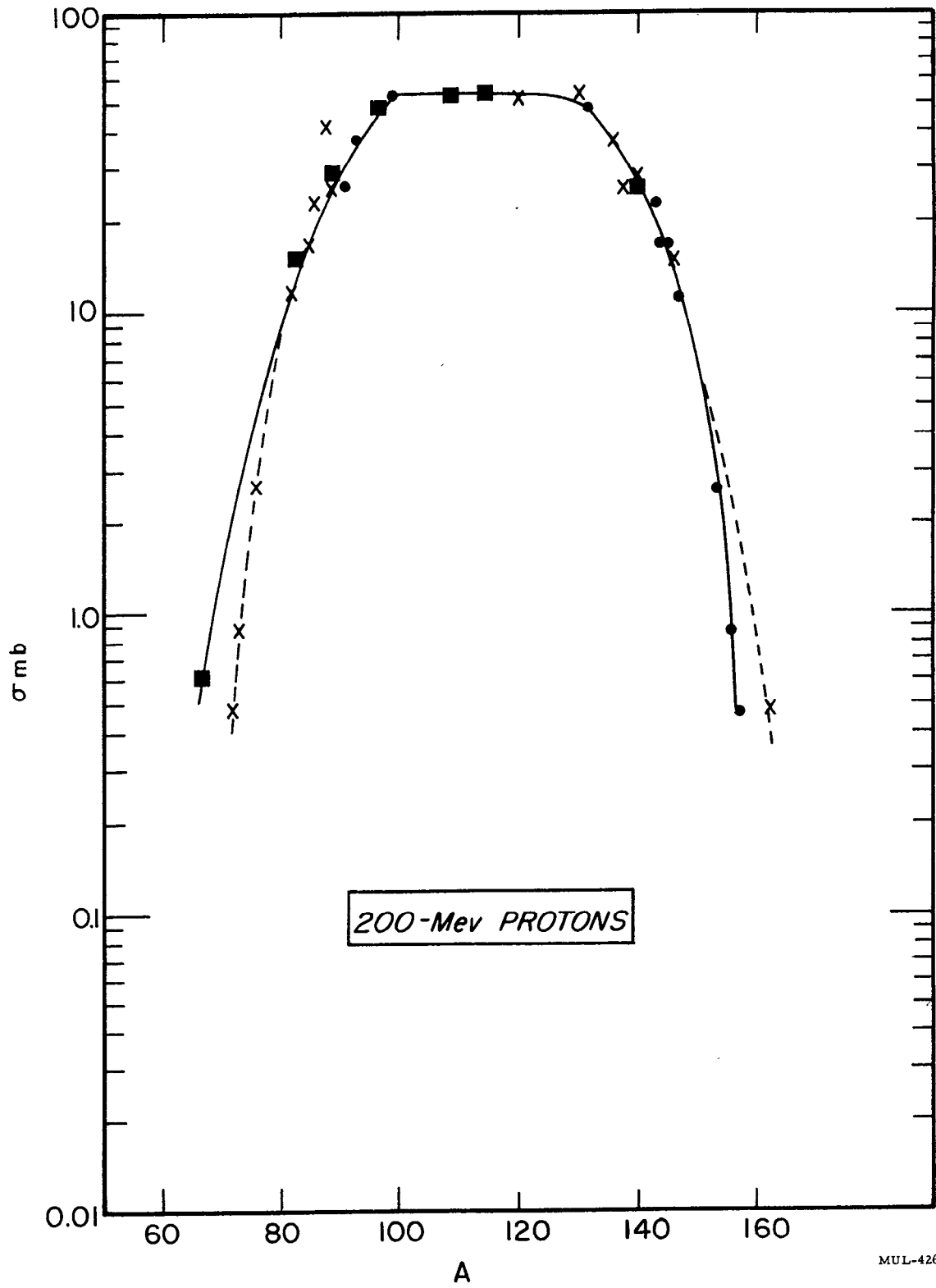


Fig. 1 F. 200-Mev Protons

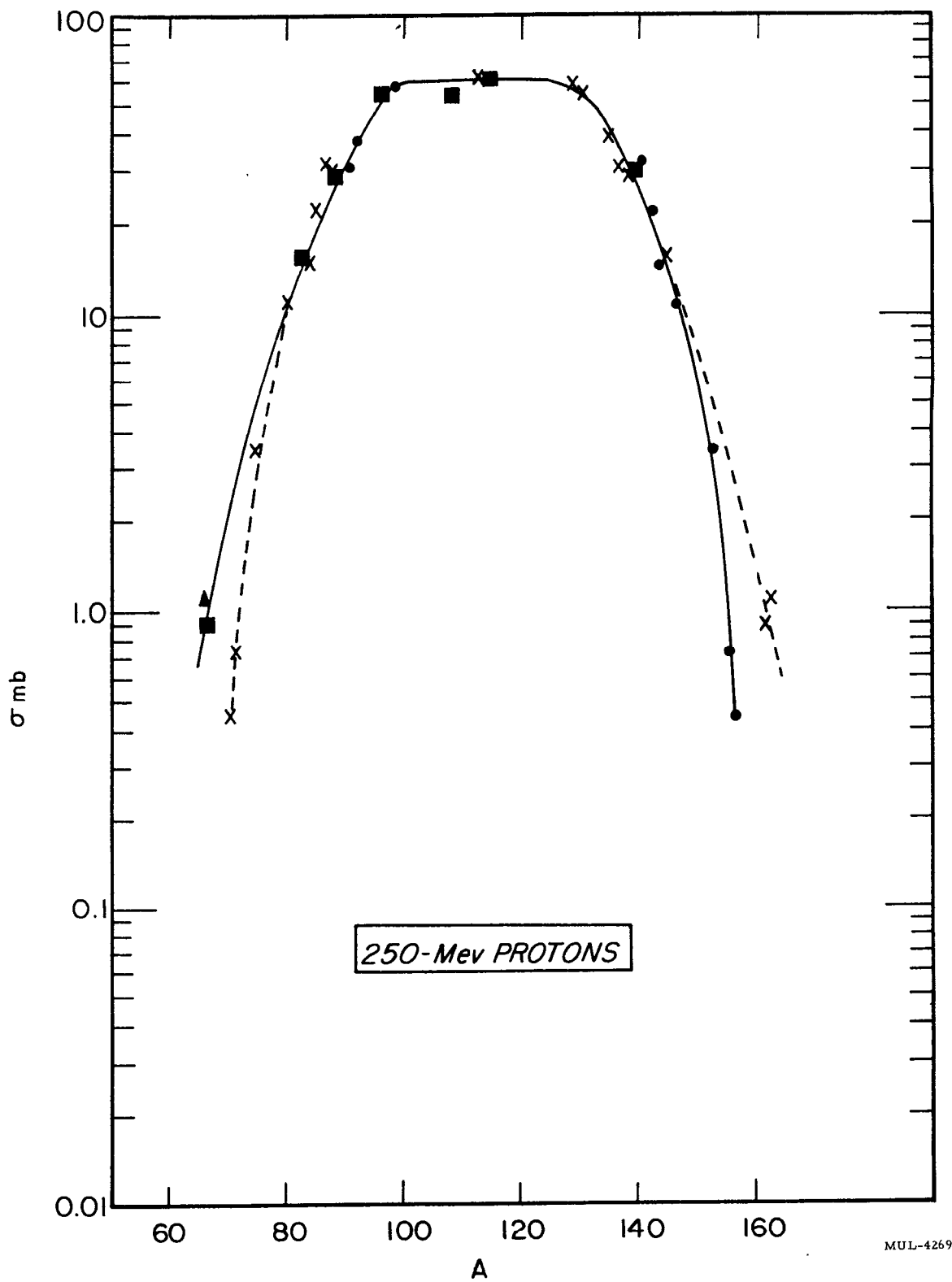


Fig. 1 G. 250-Mev Protons

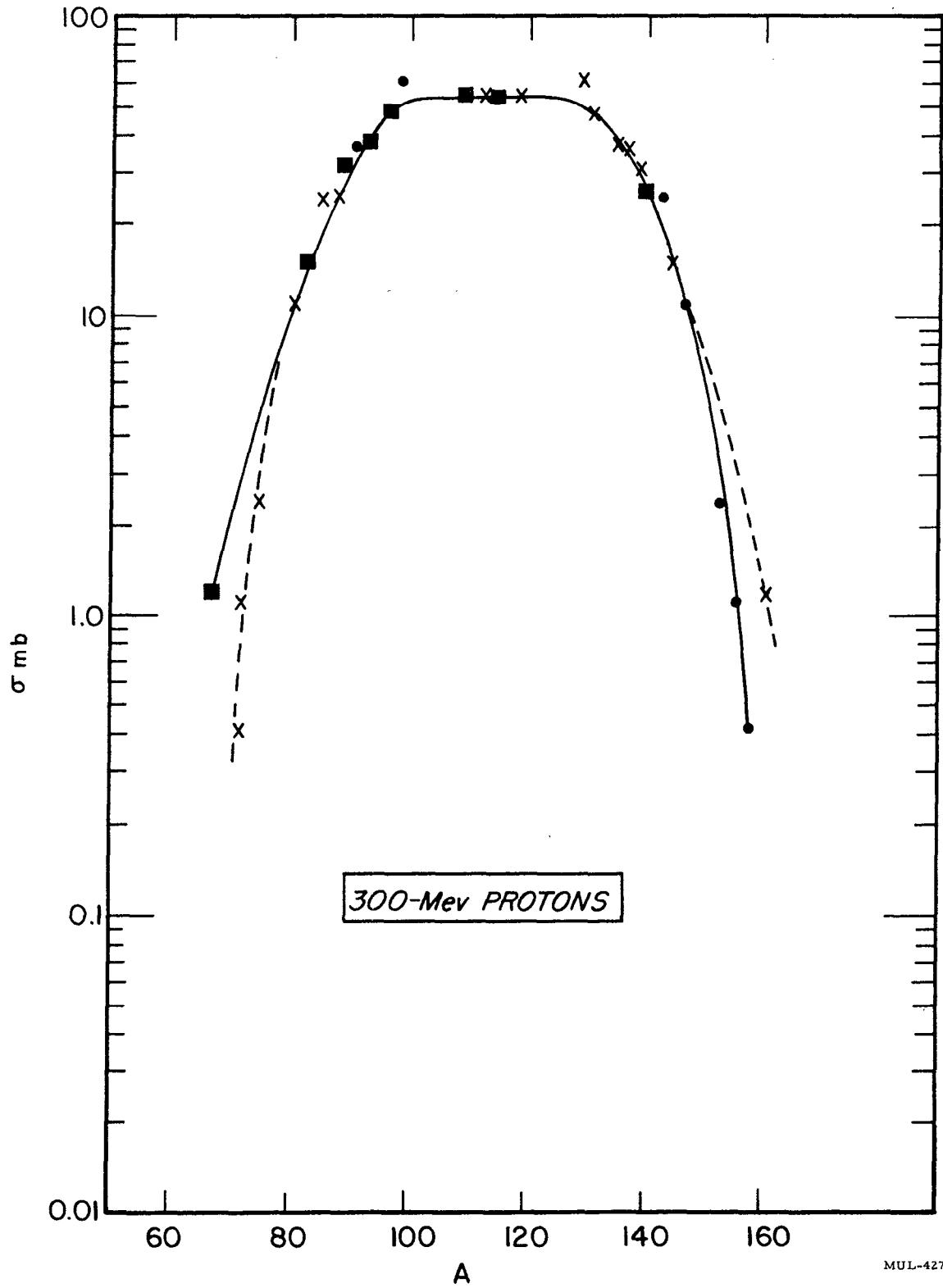


Fig. 1 H. 300-Mev Protons

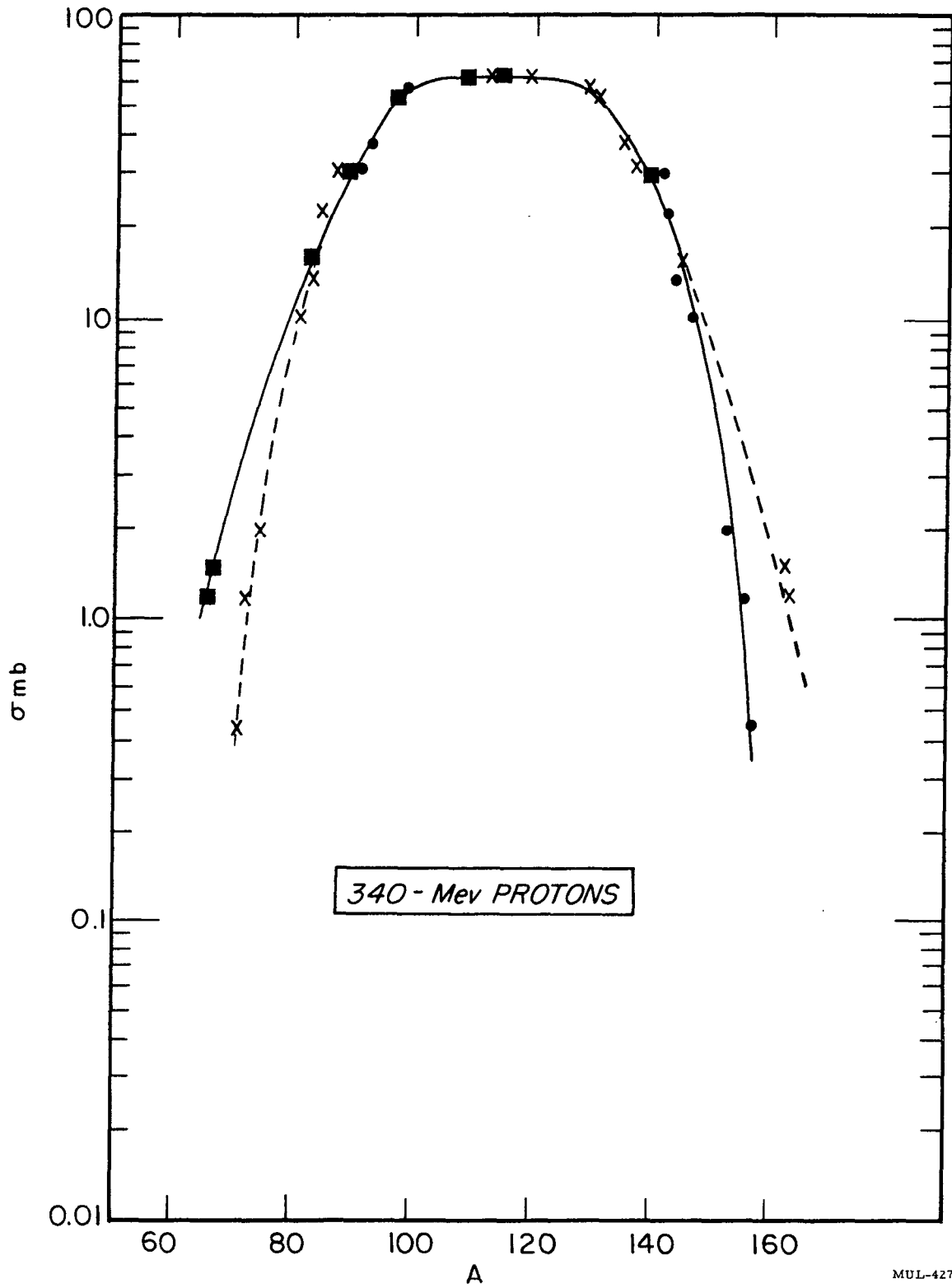


Fig. 1 I. 340-Mev Protons

MUL-4271

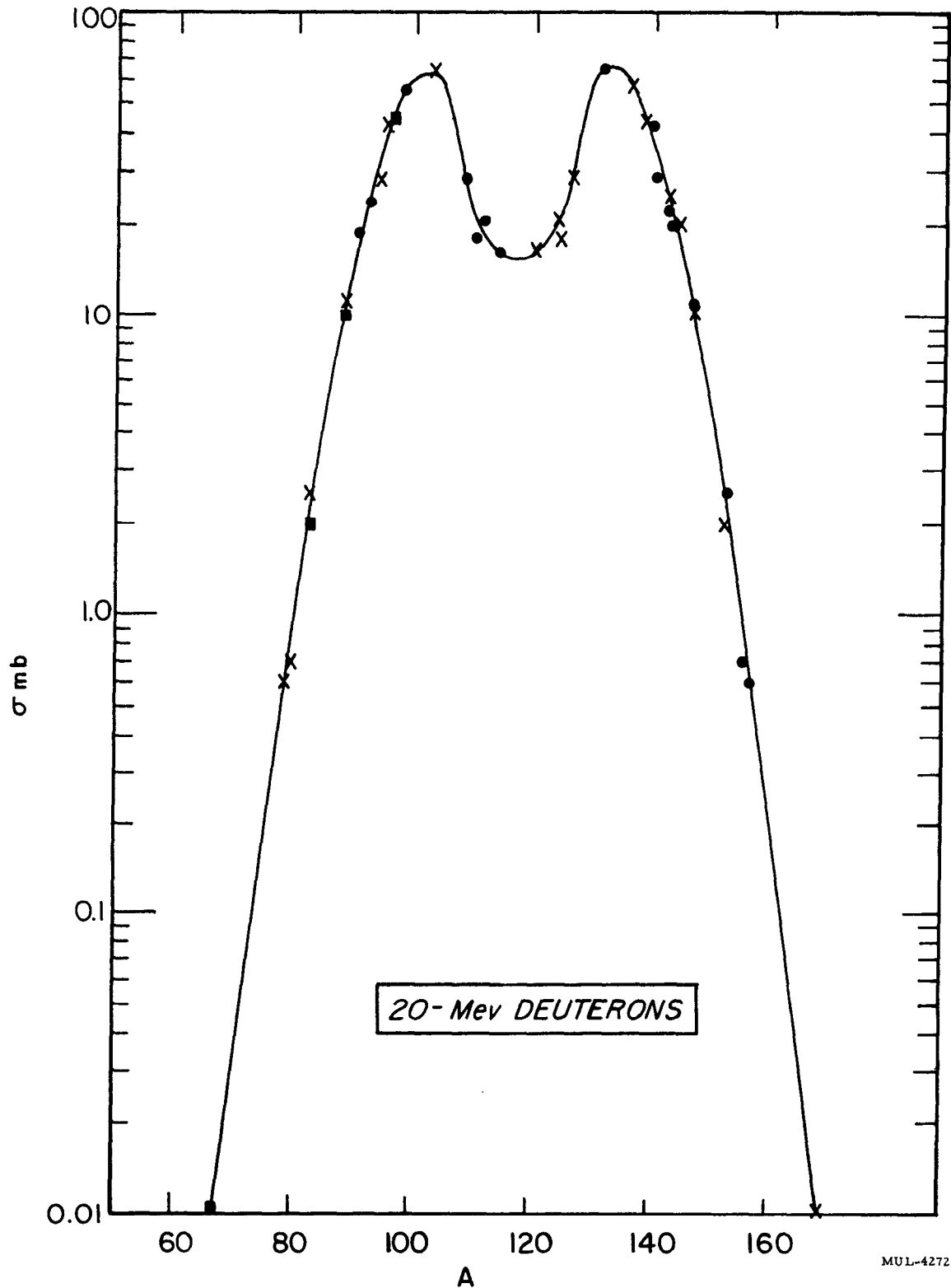


Fig. 2 A. 20-Mev Deuterons

Fig. 2. Fission-product distributions of  $U^{238}$  bombarded with deuterons of various energies. The symbol ● denotes present work; ■ denotes previous work by Hicks, Stevenson, Gilbert, and Hutchin;<sup>1,2</sup> ▲ denotes work by Lindner and Osborne;<sup>8</sup> and × denotes reflection points.

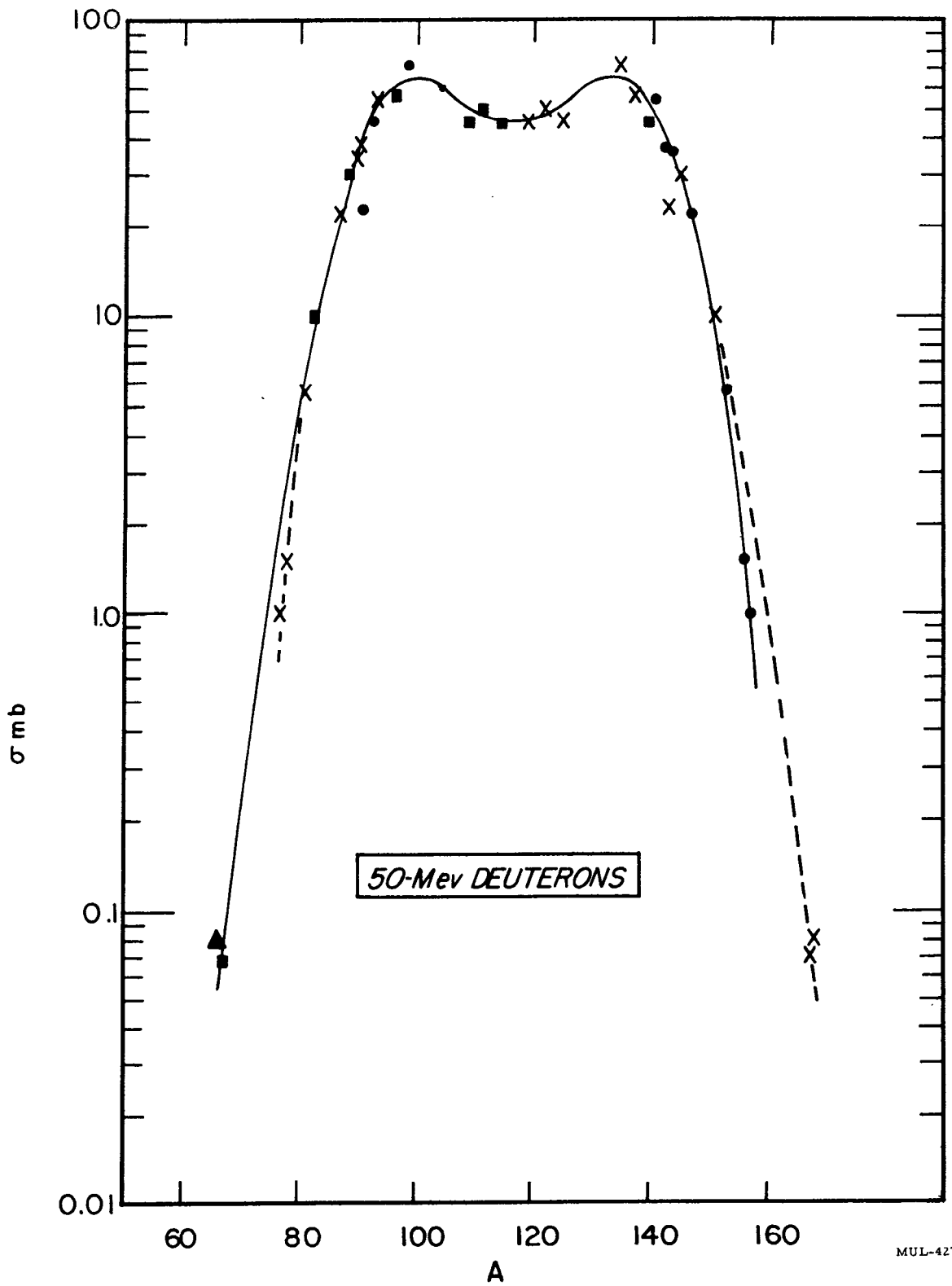


Fig. 2 B. 50-Mev Deuterons

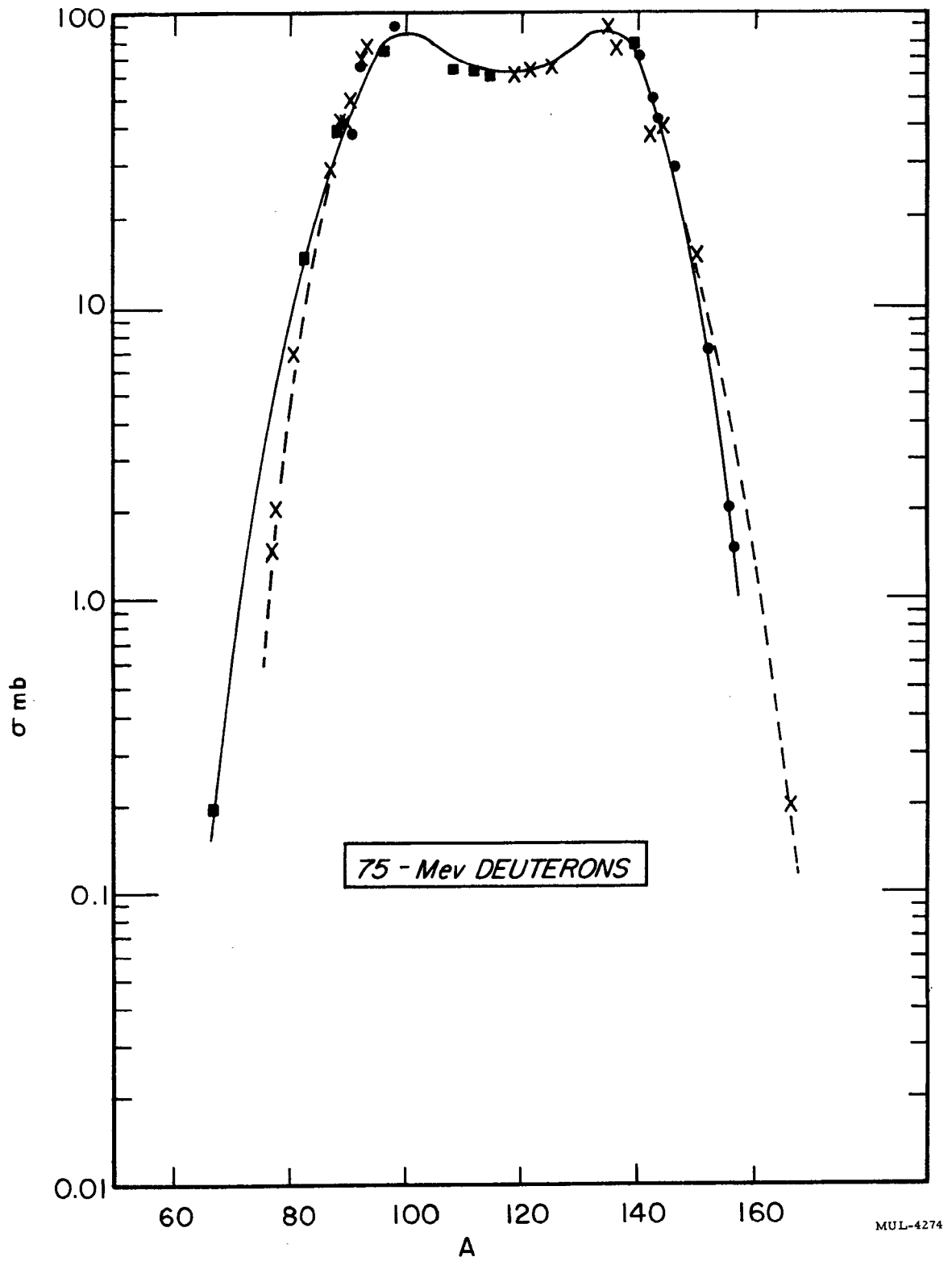


Fig. 2 C. 75-Mev Deuterons

MUL-4274

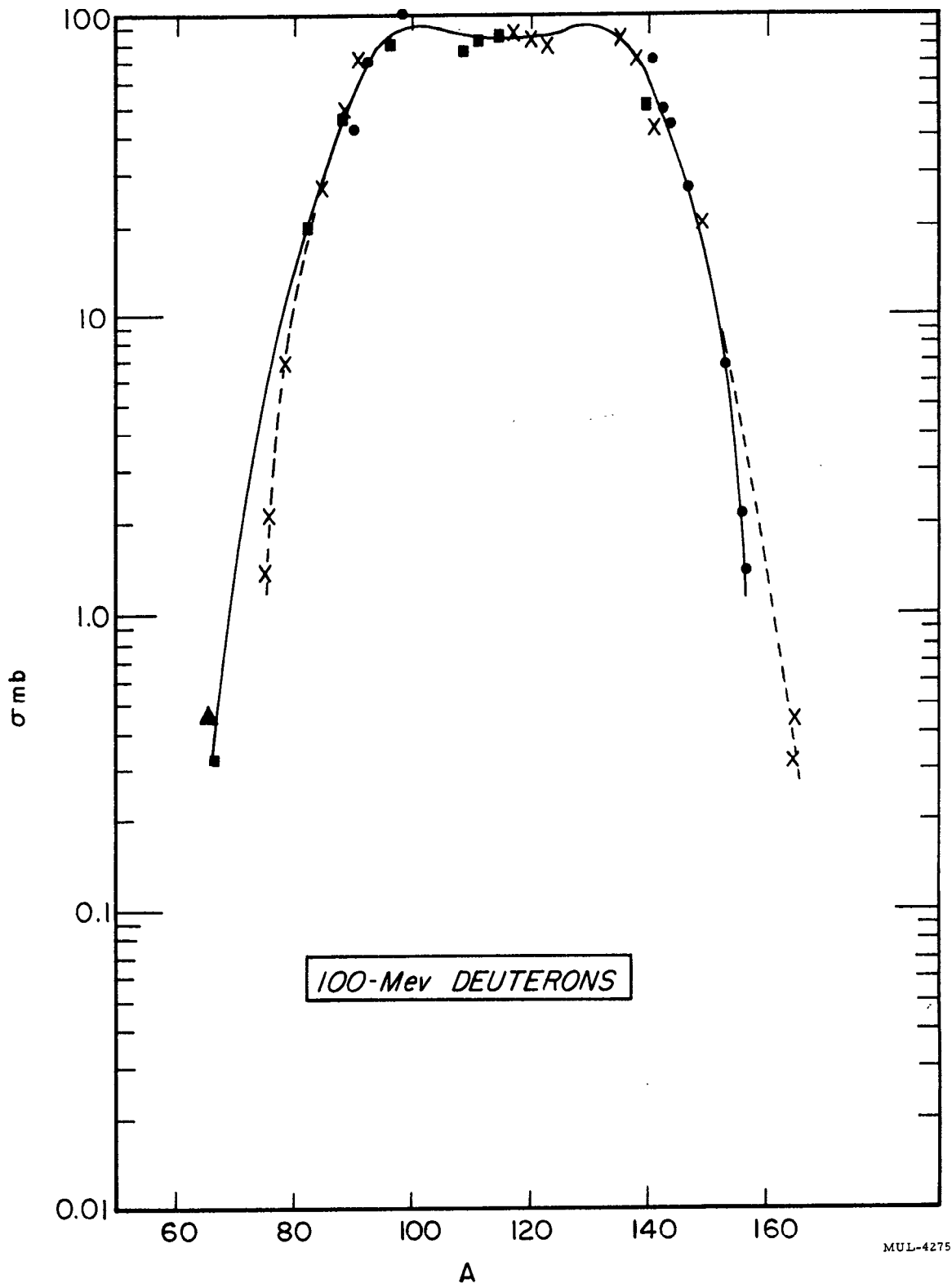


Fig. 2 D. 100-Mev Deuterons

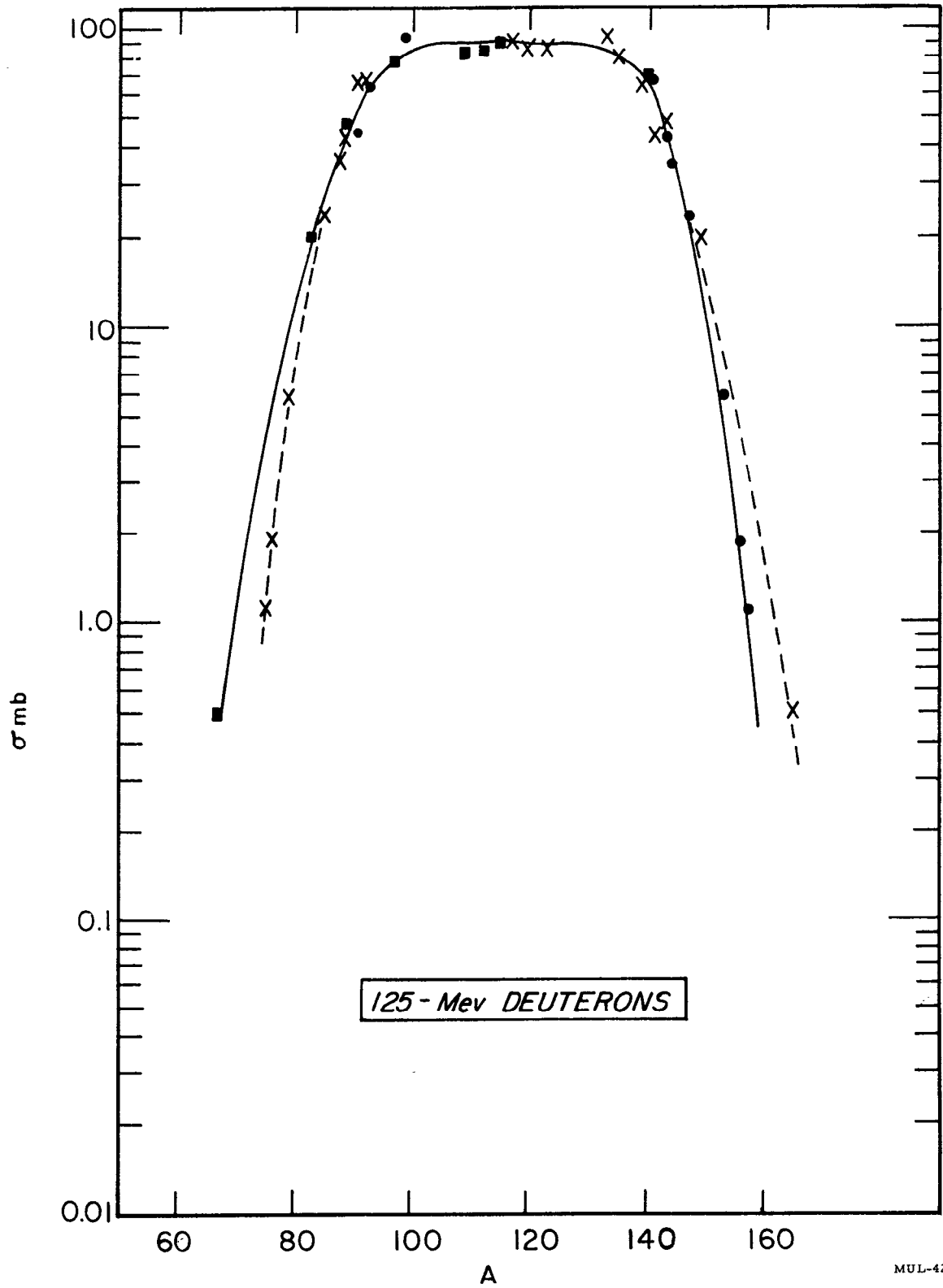


Fig. 2 E. 125-MeV Deuterons

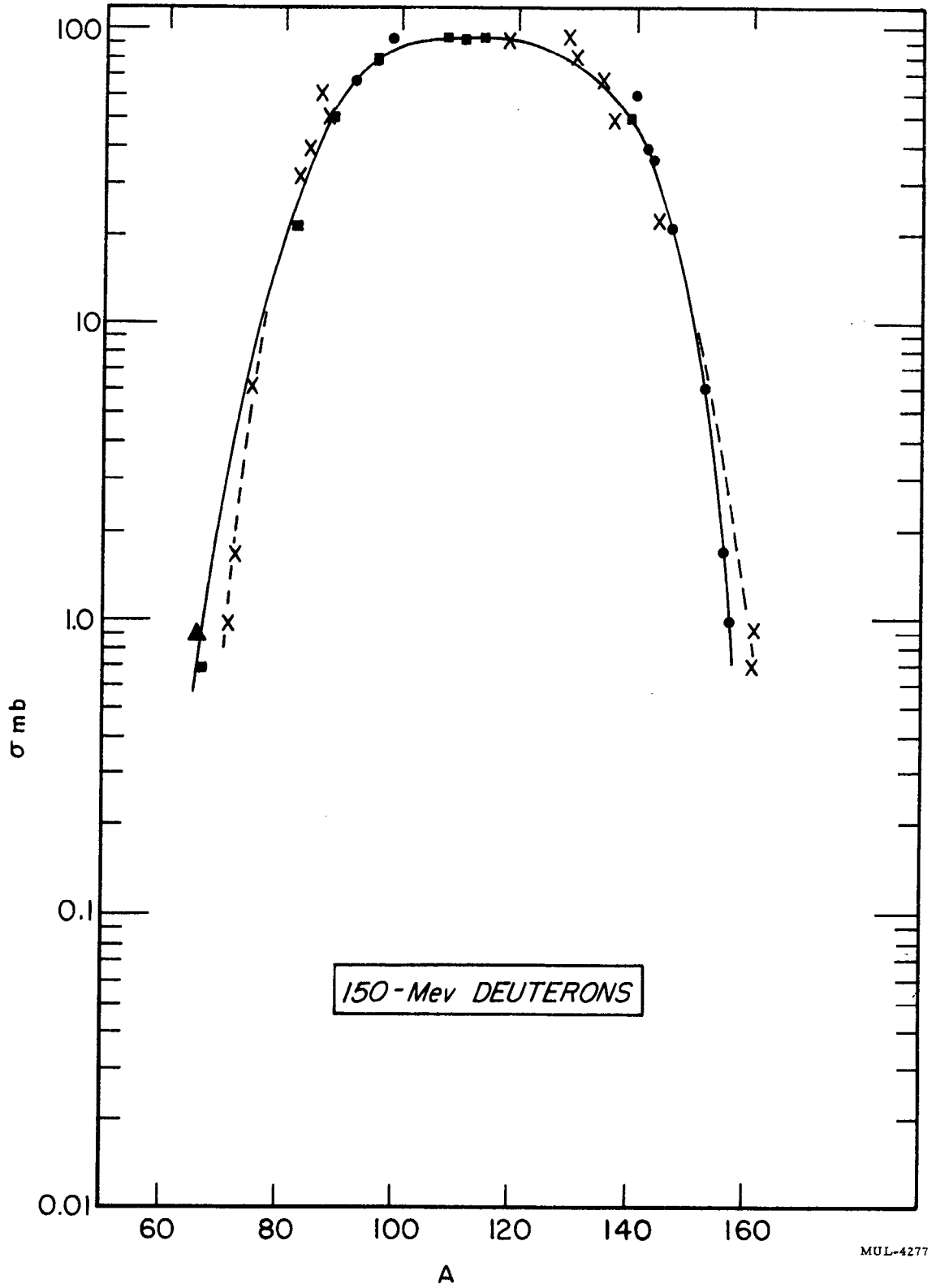


Fig. 2 F. 150-Mev Deuterons

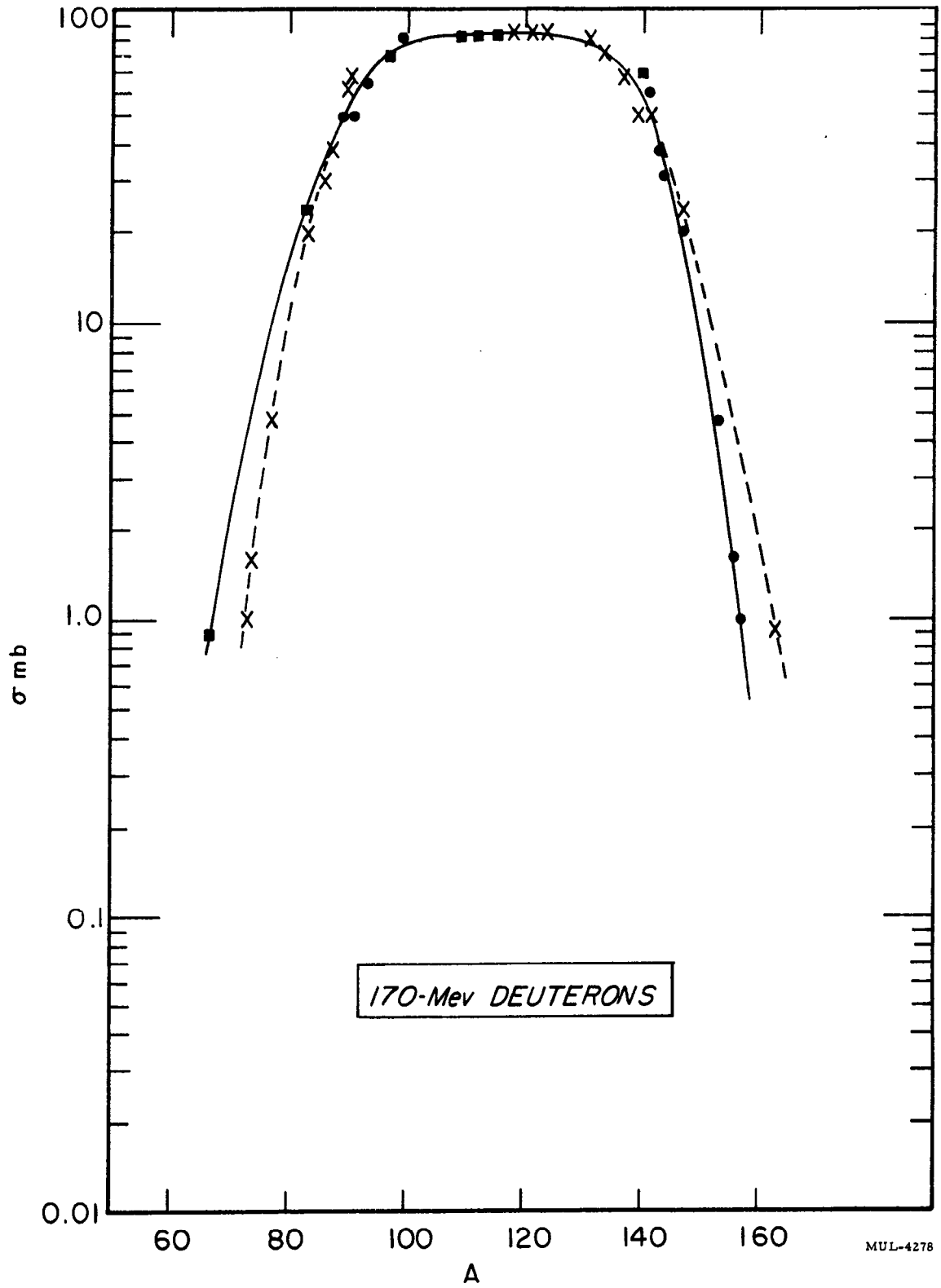


Fig. 2 G. 170-Mev Deuterons

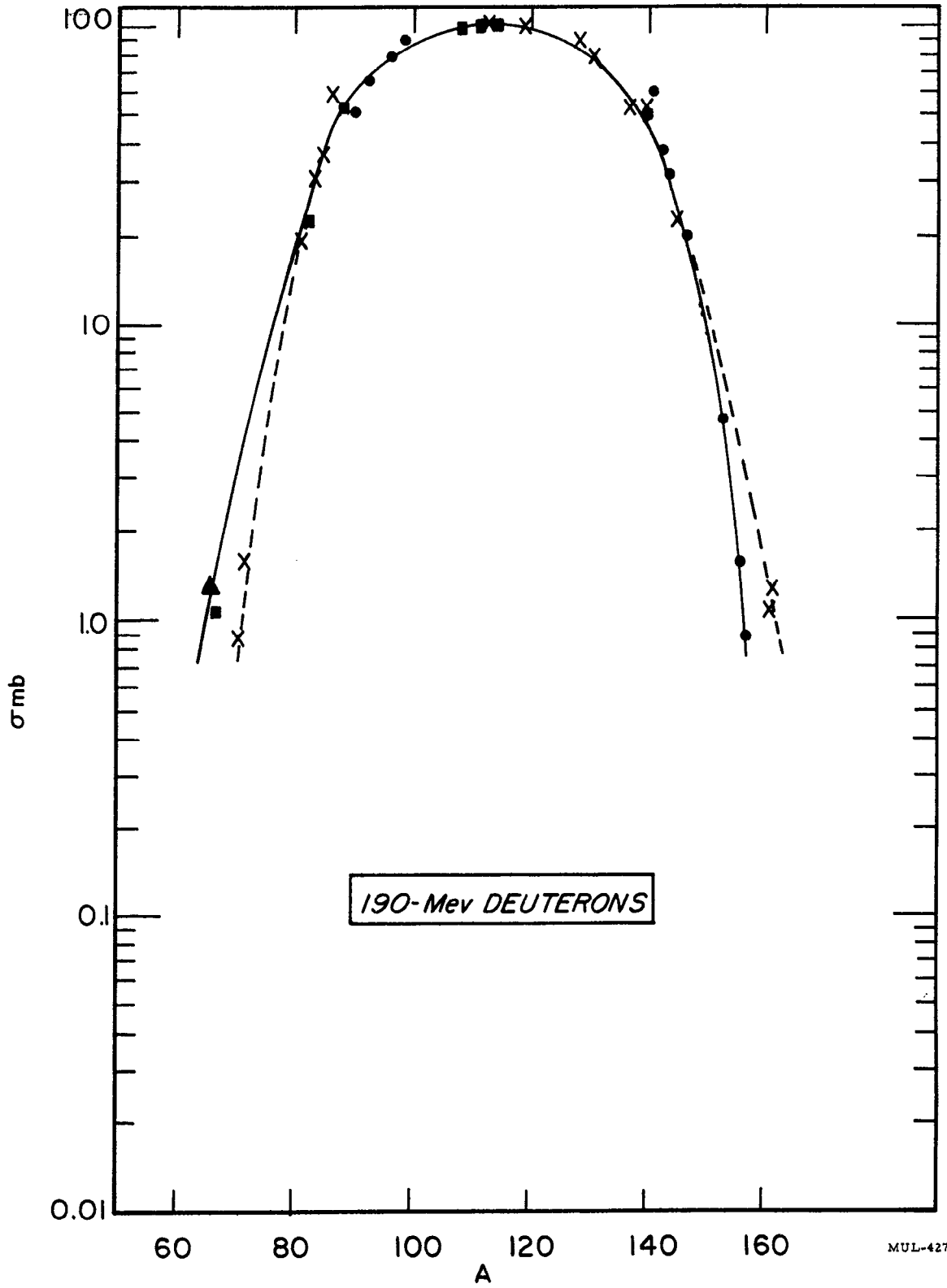


Fig. 2 H. 190-Mev Deuterons

MUL-4279

Table I. Formation cross sections in millibarns for products of  $U^{238}$  fission with protons.

Energy (Mev)	10	32	70	100	150	200	250	300	340
Nuclide									
$Y^{90}$ (a)	--	0	0.02	0.11	0.15	3.7	3.8	3.9	7.2
$Y^{91}$	0.34	27	27	50	27	26	37	37	32
$Y^{93}$	0.80	43	--	49	39	38	38	38	38
$Mo^{99}$	1.9	62	71	69	55	53	58	62	59
$La^{140}$ (a)	--	2.3	8.8	3.6	7.9	6.2	7.3	7.0	5.5
$Ce^{141}$	1.7	48	49	51	36	36	--	--	31
$Ce^{143}$	1.2	45	36	31	22	21	21	23	20
$Pr^{143}$ (a)	0	0	0.36	2.1	2.0	1.9	2.2	2.3	1.9
$Ce^{144}$	1.1	35	30	28	18	17	--	--	14
$Nd^{146}$ (b)	--	--	0	0	0.7	3.4	7.1	13	17
$Nd^{147}$	0.60	17	17	18	12	11.3	11.4	10.8	9.7
$Sm^{153}$	0.12	4.2	4.6	4.4	3.1	2.6	2.6	2.4	2.0
$Eu^{156}$	0.02	1.12	1.22	1.31	0.93	0.86	0.92	1.12	1.22
$Eu^{157}$	0.02	0.69	0.90	0.89	0.64	0.46	0.47	0.42	0.40

(a) Independent formation cross section

(b) Relative values, i. e., the counting efficiency is unknown

Table II. Formation cross sections in millibarns for products of  $U^{238}$  fission with deuterons.

Energy (Mev)	20	28	50	75	100	125	150	170	190
Nuclide									
$Y^{90}$ (a)	---	0	< 0.01	0.083	0.55	1.4	2.1	2.8	3.4
$Y^{91}$ (a)	---	20	4.7	9.5	10	11	12	12	12
$Y^{91}$	19	20	22	38	42	45	48	50	51
$Y^{93}$	24	25	46	65	71	65	62	65	68
$Mo^{99}$	55	60	68	92	101	97	92	92	92
$La^{140}$ (a)	---	0.44	4.0	10	12	12	10	11	11
$La^{141}$	28	30	54	71	67	59	50	53	53
$Ce^{141}$ (a)	---	0	0	0	4.5	8.0	8.5	7.0	6.5
$Ce^{143}$	22	28	37	49	46	40	36	35	35
$Pr^{143}$ (a)	---	0	0	0.52	1.5	2.7	2.9	3.2	3.1
$Ce^{144}$	20	25	33	43	39	32	28	29	28
$Nd^{140}$ (b)	---	< 0.2	< 0.2	< 0.2	< 0.2	< 0.2	0.5	1	3
$Nd^{147}$	11	12	22	29	27	24	21	20	20
$Sm^{153}$	2.5	2.7	5.7	7.2	7.0	6.0	5.0	4.8	4.7
$Eu^{156}$	0.60	0.67	1.5	2.0	2.1	1.9	1.6	1.6	1.6
$Eu^{157}$	0.50	0.61	1.0	1.5	1.4	1.1	1.0	1.0	0.87

(a) Independent formation cross section

(b) Relative values, i. e., the counting efficiency is unknown

### III. DISCUSSION OF RESULTS

The data (Figs. 1 and 2 and Tables I and II) show features reported by previous authors.<sup>1,2,5-13</sup> As the bombarding energy increases, modes of fission that are extremely improbable in low-energy-induced fission become increasingly important. This results in an increase of fission yield for species formed by symmetric fission and for extremely asymmetric fission, as well as increased direct formation of species near or even on the light mass side of the beta-stability region.

In drawing smooth curves through the observed fission yield values, an interesting phenomenon was observed. Below 50-Mev proton or deuteron energy the curves are symmetrical in all respects. Above 50 Mev, however, they are very definitely not symmetrical. Reflection of the heavy rare-earth cross sections through the "apparent center of the fission yield curve" as estimated from higher-yield products gives points that fall well below the observed values on the low-mass-number wing of the curve. On the other hand, reflection of the low-mass-number cross sections through the same "apparent center" mass  $A$  gives points that fall above the observed rare-earth values. The higher the energy of the bombarding particle, the more pronounced the effect. The cross sections of  $\text{Cu}^{67}$  and  $\text{Ni}^{66}$  with 340-Mev protons, for example, must be adjusted downward by at least an order of magnitude, or those of  $\text{Eu}^{156}$  and  $\text{Eu}^{157}$  adjusted upward by factors of from three to seven, in order to fall on a curve symmetric about a single  $A$ . Duplicate runs of  $\text{Eu}^{156}$  and  $\text{Eu}^{157}$  cross sections showed agreement within five percent while the cross sections of  $\text{Cu}^{67}$  and  $\text{Ni}^{66}$  were from independent investigations.<sup>8</sup> The effect is certainly outside of experimental error.

The phenomenon described above might conceivably come about if a major portion of the independent yields of the rare-earth nuclides arose from direct formation either as stable isotopes or on the neutron-deficient side of stability. If the primary fission products of mass 156, for instance, were distributed so that 75-80% of the mass yield lay in the region where

<sup>9</sup> R. W. Spence and G. P. Ford, *Ann. Rev. Nuclear Sci.* **2**, 399 (1953).

<sup>10</sup> R. H. Goeckermann and I. Perlman, *Phys. Rev.* **76**, 628 (1949).

<sup>11</sup> P. R. O'Connor and G. T. Seaborg, *Phys. Rev.* **74**, 1189 (1948).

<sup>12</sup> R. L. Folger, P. C. Stevenson, and G. T. Seaborg, *Phys. Rev.* **98**, 107 (1955).

<sup>13</sup> E. M. Douthett and D. H. Templeton, *Phys. Rev.* **94**, 128 (1954).

$Z \geq 64$  (Gd or higher), then the fission yield curves could be considered to be symmetric. This situation appeared unlikely, for only one neutron-deficient species ( $\text{Nd}^{140}$ ) was detected in the entire rare-earth region. More conclusively, if the major portion of the yield of mass 156 lay in the region of  $Z \geq 64$ , then the direct-formation cross section of  $\text{Eu}^{156}$  should have been of magnitude comparable to or larger than that of  $\text{Sm}^{156}$ . Measurement of the direct-formation cross section of  $\text{Eu}^{156}$  showed that over 90% of the  $\text{Eu}^{156}$  was formed from its  $\text{Sm}^{156}$  parent by beta decay. Thus, the fission yield distribution above 50 Mev is not symmetrical.

The fission cross sections shown in Figs. 3 and 4 and Table III were obtained by integration under the fission-yield curves. Also shown are the data of previous workers.<sup>14, 15, 16</sup> The differences between the present work and that of reference 2 reflects the error of the assumption that the fission-product distribution is symmetrical.

Table III.  $\text{U}^{238}$  fission cross sections, in barns.

Protons		Deuterons	
Energy (Mev)		Energy (Mev)	
10	0.029	20	1.03
52	1.47		
70	1.47	50	1.61
100	1.49	75	2.13
150	1.44	100	2.42
200	1.47	125	2.45
250	1.56	150	2.39
300	1.46	170	2.48
340	1.59	190	2.49

<sup>14</sup> J. A. Jungerman, Phys. Rev. 79, 632 (1950).

<sup>15</sup> H. M. Steiner and J. A. Jungerman, Phys. Rev. 101, 807 (1956).

<sup>16</sup> G. N. Harding, Atomic Energy Research Establishment Report No. AERE/NR-1456, Harwell, Berks., Engl., June 1954 (unpublished).

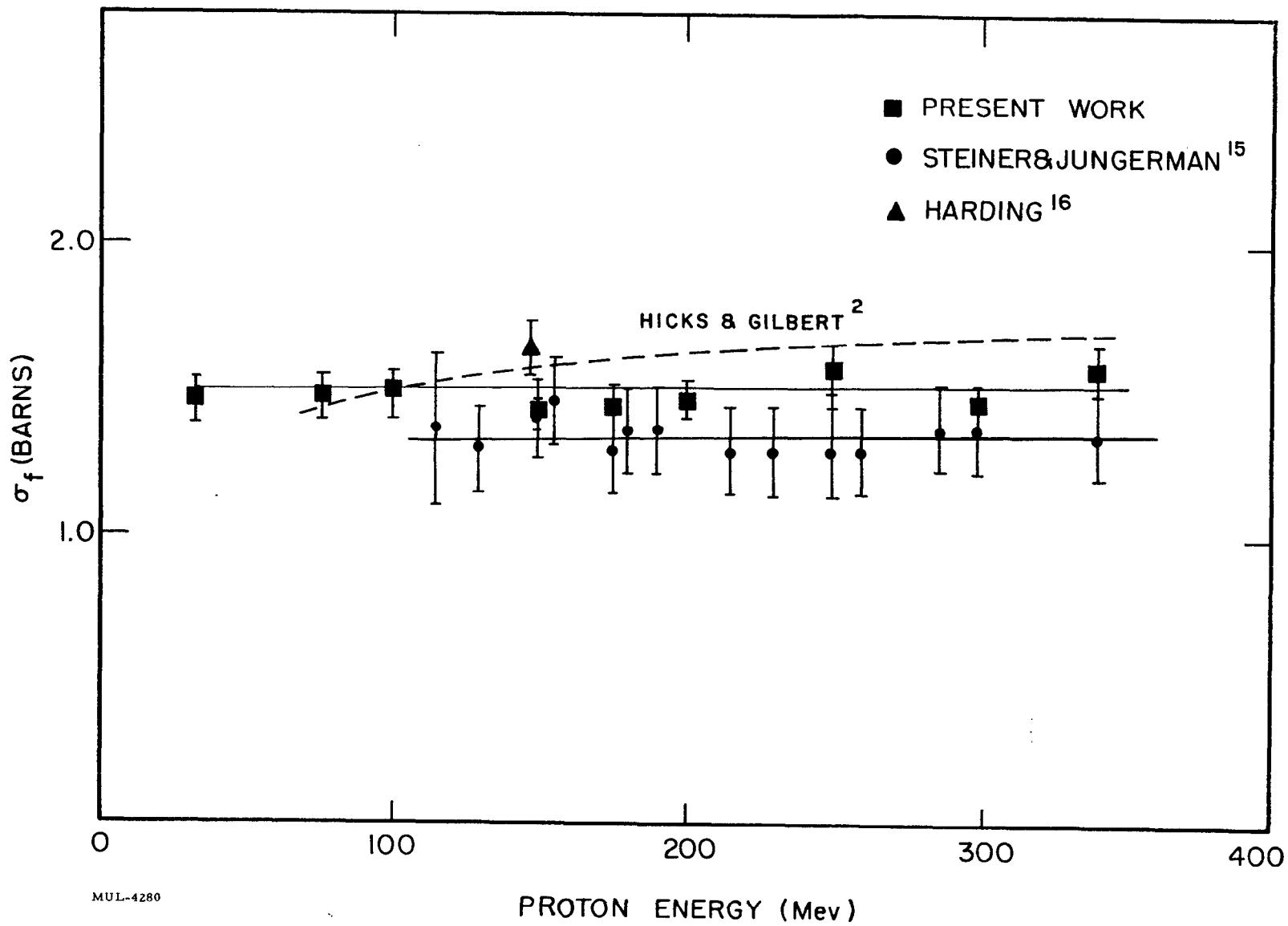


Fig. 3. Fission cross section of  $U^{238}$  bombarded with protons of various energies.

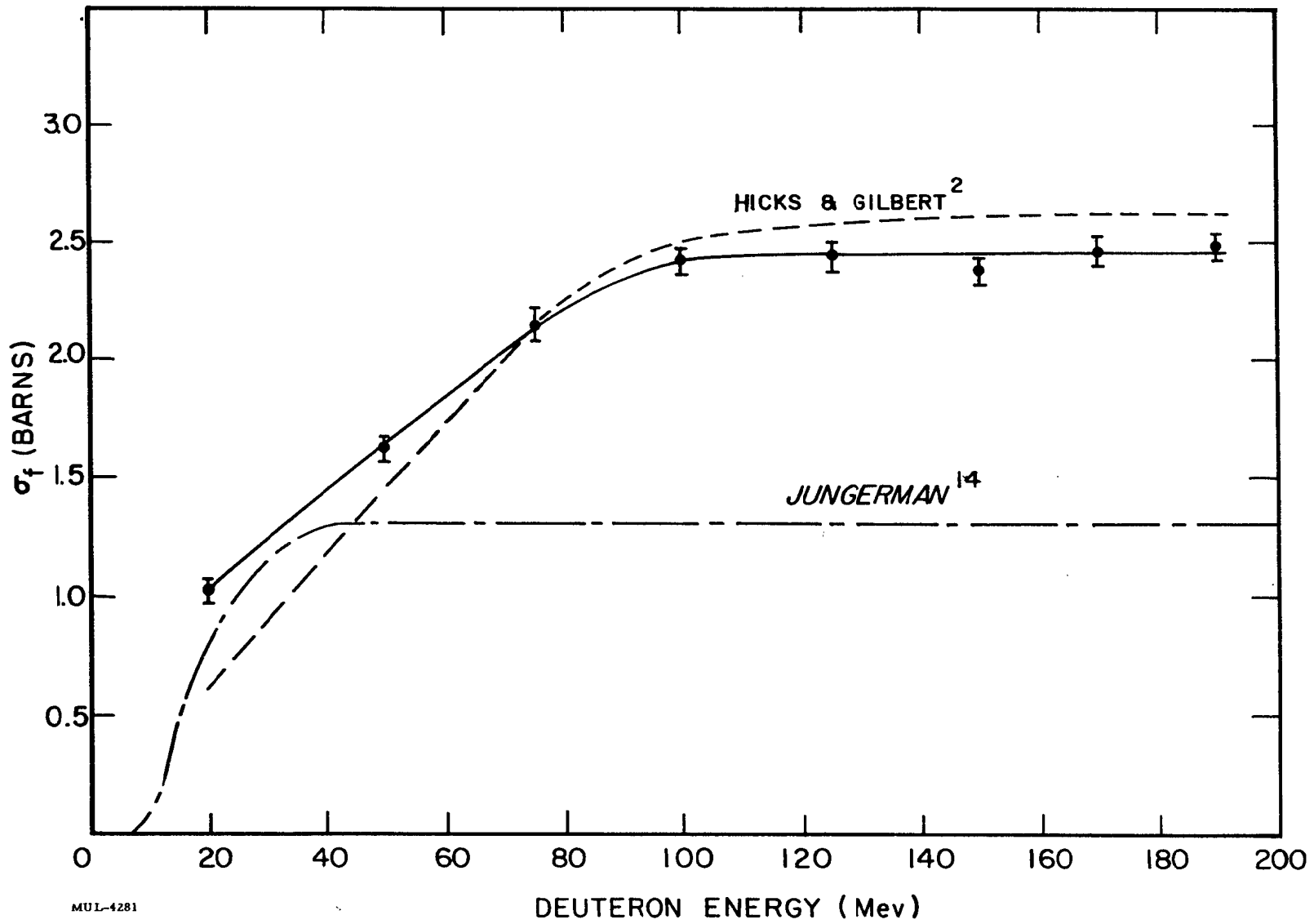


Fig. 4. Fission cross section of  $U^{238}$  bombarded with deuterons of various energies.

As the energy of the bombarding particles is increased above 30-40 Mev, the mean free path of the projectile in nuclear matter becomes comparable to the diameter of the target nucleus, rendering the nucleus partially transparent to high-energy nucleons.<sup>17</sup> The picture of "compound nucleus" formation must be abandoned, and collisions of the projectile with individual nucleons in the target nucleus must be considered. In each of the collisions, the energy transfer to the nucleus is a fraction of the projectile energy. The total energy transferred to the nucleus then depends on the number of collisions the projectile makes within the nucleus and may vary from the full energy of the projectile to a small fraction thereof.

Monte Carlo calculations by Turkevich on the deposition of energy in the Bi<sup>209</sup> nucleus by protons appear in an article by Porile and Sugarman.<sup>18</sup> The results show that the majority of the interactions deposit less than half the projectile energy at 286 and 458 Mev.

When the transfer of energy to the nucleus is small, comparatively few nucleons are evaporated either before or after fission and the sum of the complementary-fragment mass numbers is close to 238. Similarly, when the energy transfer is large, the system evaporates many nucleons, predominately neutrons, and the sum of the complementary-fission-fragment mass numbers is much less than 238. The lower-energy fission events are characterized by a saddle in the central region ( $A \sim 118$ ) of the distribution curve symmetric about a given  $A$ , and by very steep sides in the low- and high- $A$  regions. As the bombarding energy increases, the valley disappears and the low- $A$  wing has a lower slope than the high- $A$  wing. From the character of the fission yield distribution at higher energies, one may infer that for "mono-energetic" high-energy fission the valley has all but disappeared and the axis of symmetry of the distribution has shifted toward lower  $A$ . The measured distribution is, of course, a mixture of both high- and low-energy events. The fission-yield distributions in Figs. 1 and 2 display apparent symmetry about a central mass number  $A$  in the region of  $A \pm 20$  at all energies. These products are major yields of both high- and low-energy fission. Thus, almost any

---

<sup>17</sup> R. Serber, Phys. Rev. 72, 1114 (1947).

<sup>18</sup> N. T. Porile and N. Sugarman, Phys. Rev. 107, 1422 (1957).

combination of fission-yield distributions would tend to produce a slowly varying curve in this region. The products in apparent complementary positions with respect to the observed distribution are not necessarily complementary fragments of every individual fission process. The observed yields of these products are nearly the same; therefore, any discrepancies are small and tend to be averaged out.

Those nuclides on the light-mass wing of the distribution ( $A \leq 75$ ) are seen in appreciable yield only in high-energy-induced fission, in particular,  $\text{Cu}^{67}$  and  $\text{Ni}^{66}$ , which are not seen in thermal-neutron or low-energy charged-particle induced fission. At 340-Mev protons, the cross sections of masses 66 and 105 are equal. Therefore, the fissioning nucleus giving rise to  $A = 66$  must have had enough excitation energy to lose many nucleons either before or after scission. The sum of the fission-fragment masses must be not greater than 221, and probably at least two mass units less.

On the other hand, those nuclides on the heavy-mass wing are seen in low-energy fission. The fission yield of  $\text{Eu}^{136}$  varies but slightly (from 0.06 to 0.09%) over the entire energy range of charged particles used. The slopes of all fission-product distributions in the region  $A \geq 100$  (Figs. 1 and 2) are very nearly identical at all charged-particle energies used in this work.

#### IV. ACKNOWLEDGMENTS

We wish to thank Mrs. Nancy Lee and Mrs. Joyce Gross for technical assistance; Mr. J. T. Vale and the crew of the 184-inch cyclotron, and the late Mr. G. B. Rossi and the crew of the 60-inch cyclotron for their cooperation in making the bombardments possible.